Isı Bilimi ve Tekniği Dergisi, 40, 1, 77-86, 2020
J. of Thermal Science and Technology

ISSN 1300-3615

CFD INVESTIGATION OF THE NEAR-SURFACE STREAMLINE TOPOLOGY ON A SIMPLE NONSLENDER DELTA WING

Haci SOĞUKPINAR[*], Serkan ÇAĞ[**] and Bülent YANIKTEPE[***]
* University of Adıyaman, Department of Electric and Energy, Vocational School, Adıyaman 02040, Turkey hsogukpinar@adiyaman.edu.tr
** University of Adıyaman, Department of Machinery and Metal Technology Vocational School,02040, Turkey, scag@adiyaman.edu.tr
*** Korkut Ata University, Department of Energy Systems Engineering, Faculty of Engineering, Osmaniye, 80000, Turkey, byaniktepe@osmaniye.edu.tr

(Geliş Tarihi: 27.02.2019, Kabul Tarihi: 18.02.2020)

Abstract: In this study, a non-slender simple delta wing was investigated numerically by using RANS with SST $k-\omega$ turbulence model and the results were compared with experimental data to validate the simulation accuracy of the Computational Fluid Dynamics (CFD) approach. The delta wing configuration has a straight wing, with thickness 3 mm, chord length 101.6 mm, wingspan 254 mm, 30° beveled angle, and 40° sweep leading edge. Effect of angle of attack on the near-surface patterns of the delta wing was interpreted in terms of streamline topology, particularly bifurcation lines, as well as contours of streamwise and transverse velocity components, and also vorticity contours on the surface at the angle of attack starting from 5° to 17° with Reynolds number of $1x10^4$. The leading-edge vortices (LEV) developed at the angle of 5°, the vortex breakdown happened first time at the angle of 7° and moved upstream direction and reached around x=0.5c at 10°. With the increasing angle of attack further, vortex breakdown moved to upstream a substantial distance and finally, the stall occurred at an angle of attack at 17°.
Keywords: LEV, CFD, SST, delta wing, vorticity, leading-edge vortices.

HESAPLAMALI AKIŞKANLAR DİNAMİĞİ KULLANILARAK BASİT ÜÇGEN KANAT MODELİNDE YAKIN YÜZEY AKIŞ YAPISININ İNCELENMESİ

Özet: Bu çalışmada, düşük süpürme açısına sahip basit üçgen kanat modeli RANS denklemleri kullanılarak SST k-ω türbülans modeli ile incelenmiş, elde edilen bulgular daha önceden yapılmış deneysel verilerle kıyaslanarak Hesaplamalı Akışkanlar Dinamiğinin (HAD) tutarlılığı doğrulanmaya çalışılmıştır. Bu çalışma için, kiriş uzunluğu 101,6 mm, kanat genişliği 254 mm, et kalınlığı 3 mm, pah açısı 30°, ve süpürme açısı 40° olan üçgen kanat modellenmiştir. Hücum açısının (5 dereceden 17 dereceye kadar) kanat yüzeyi üzerindeki akış yapısına etkisi ve girdap çökmesi, hem üst plan hem de arka plan görüntüsü açısından Reynolds sayısı 10.000'de sabit tutularak incelenmiştir. Kıvrımlı, hücum kenar yanal girdap oluşumu 5 derecede başlamış, girdap çökmesi ilk defa 7 derecelik hücum açısında kanadın arka kısmında oluşmuş ve 10 derecede kanadın ön tarafına (x/c=0.5) doğru ilerlemiştir. Hücum açısı artıkça girdap çökmesi kanadın ön uç kısmına ilerlemiş, yaklaşık 17 derecede akış stol olmuştur.
Anahtar kelimeler: LEV, CFD, SST, üçgen kanat, girdap, hücum kenar yanal girdap.

INTRODUCTION

Unmanned aerial vehicles (UCAV) were developed as reconnaissance vehicles, and even as tactical weapons mostly in military applications but nowadays, commercial usage has been expanding to scientific, agricultural, and other applications such as policing, peacekeeping, agriculture, and smuggling. Therefore a non-slender or 'low sweep' (Λ<60) delta wings has become a very important topic to investigate in the last 3 decades. The typical and well-known delta wing flow is the formation of Leading-Edge Vortices (LEV) which has determined across a wide range of Reynolds numbers and varying angle of attacks. This flow separates at a low angle of attack and the separated layer rolls up to form a large-scale

vortex on each half of the wing. Flow regime on a non-slender delta wing was investigated experimentally and numerically then primary characteristics of the flow structure and the potential for their control were summarized. It is difficult to observe vortex breakdown at high Reynolds numbers (10^6) (Wentz and Kohlman, 1971) but the well defined vortical flow was clearly visible at low Reynolds numbers of 7000 (Ol and Gharib, 2003). Experimental evidence suggests that as the increasing Reynolds number, vortex breakdown moves apex (Elkhoury *et al*.,2005) even at a small angle of incidence. The location of vortex breakdown also depends on the angle of incidence therefore with the increasing angle of attack, the onset of vortex breakdown moves up the apex and separated shear layers become the dominant feature of the flow (Gursul *et al.,* 2005). As the increasing angle of attack further, primary attachment occurs outboard of the symmetry plane and this attachment line moves in-board towards the wing centerline where vortex breakdown and stall occur and the identification of buffeting mechanisms in these regions (Yaniktepe and Rockwell, 2004). An experimental study showed that at low Reynolds number or at low angle of attack, there is an elongated separated flow region exists which lies very close to the upper surface of the wing (Taylor *et al*., 2003) and velocity profile in numerical studies showed similar property with those experiments (Gordnier and Visbal, 2003). Numerical results indicate a broad wake-like flow that is coherent with the experiment. Flow field over a yawed simple delta wing was investigated experimentally and study indicated that there was a symmetrical flow on the delta wing in the case of zero yaw angle but with changing the angle, vortex breakdown occurs earlier on the windward side of the delta wing and vortex breakdown location moves further downstream on the leeward side of the delta wing (Canpolat *et al*., 2009; Yayla *et al*., 2010). They observed high-scale Kelvin-Helmholtz vortex structure at side view which was emanating from the leading edge to rolls up periodically into discrete sub-structures especially at the angle of 13° and 17°.Another experiment shows the presence of a co-rotating form of small scale vorticity and this was noticeable in sudden images of the flow (Yavuz *et al*., 2004). Numerical prediction and wind tunnel experiment for a pitching unmanned combat air vehicle were conducted for a modified delta wing up to the angle of attack 25° (Cummings *et al*., 2008) with various frequencies of pitch oscillation. For the numerical part Reynolds Average Navier-Stokes equations (RANS) were implemented for compressible flow and vorticity patterns were figured out. Vortex breakdown was calculated in the middle of the wing surface at the angle of 15°. Vorteks breakdown was simulated like streamline rotating and enlarging by spiral motion. Another numerical study investigated the flow field structure by using Computational Fluid Dynamic approaches (CFD) with the Shear Stress Transport (SST) model (Saha and Majumdar, 2012). Vortex breakdown phenomenon above a delta wing at high angles of attack for the cases with and without a symmetric trailing-edge jet flap was investigated by using RANS Low Reynolds Launder–Sharma k–e turbulence model (Kyriakou *et al*., 2010) but in the figures, the onset of vortex breakdown was not clearly presented. Detached-Eddy Simulation of the vortical flow field about the VFE-2 delta wing was investigated (Cummings and Schütte, 2013) and compared with available experimental data. CFD calculation was conducted with unstructured Cobalt code by using RANS, DES (Detached-Eddy Simulation), and DDES (Delayed Detached-Eddy Simulation) turbulence models. Mostly Lift, drag and pressure coefficients were calculated and compared with available experiment but the figures show only LEV structure. Vortex breakdown behind a delta wing was investigated by using a Large Eddy Simulation (LES) method and compared with wind tunnel experiments (Mary, 2003). In the paper, only numerical data were presented but plan and end view visual presentations were rarely considered. Effect of thickness-to-chord ratio on flow structure of a low swept delta wing was investigated in a low-speed wind tunnel using laser-illuminated smoke visualization, particle image velocimetry, and surface pressure measurements (Gülsaçan *et al*., 2018). The thickness of the wing was changed and its effect on the flow structure was investigated then plan and end view smoke visualization and pressure coefficient on the surface were presented and discussed. Several other experimental (Canpolat *et al*., 2011) studies were conducted to investigate the flow field regime of delta wing but the tremendous cost involved in building up of the experimental system like a wind tunnel, PIV, etc. For instance, the wind tunnel has the advantage of dealing with a ‘‘real’’ fluid and can produce global data over a far greater range of the flight envelope than CFD can (Johnson *et al*., 2005). However, CFD accelerates the design process and saves time and millions of money. Today CFD has joined the experimental process to provide significant value in vehicle design. Therefore in this study flow field characteristics of simple delta wing were investigated by using RANS with SST k-ω turbulence model and plan and end view streamline and streamwise velocity and vorticity field were investigated and location and shape of LEV and vortex breakdown were clearly presented and obtained data were compared with available experiments.

NUMERICAL APPROACH

The flow solver PARDISO (a commercial version built-in COMSOL) was chosen because of its performance, robust, memory efficient and easy to use software for solving large sparse symmetric and unsymmetrical linear systems of equations on shared-memory and distributed-memory multiprocessors (Internet, 2019). For the current study direct solver, PARDISO with nested dissection multithreaded preordering algorithm was set. Constant (Newton) nonlinear method was used for the method then iterations options were specified for termination technics. PARDISO solves the RANS equation for the SST k-ω turbulence model. This model combines the superior behavior of the k-ω model in the near-wall region with the robustness of the k-ε model (Menter, 1994). Detailed information about numerical calculation and modeling is available at (Sogukpinar, 2019, 2018, Internet, 2019). The PARDISO solved RANS equations with two turbulence equations for the incompressible flow along the simple delta wing. For the equations, gravity was included and no-slip condition was applied on the wing surface. The upstream, top and bottom border of computational domains are situated at least 10 mean aerodynamic chords away to minimize the effect of the applied boundary circumstances. The boundary conditions were set to velocity inlet and open boundary and other parts stay as a wall. Not half but the full model was simulated under wind speed of 5.6 cm/s. For the delta wing surface, the triangular mesh type was applied and the minimum mesh size was set to 0.0001 m, and 0.0005 m for the maximum. Then the model was fully enclosed in a thin ellipsoid and tetrahedral mesh type was preferred with a maximum growth rate of 1.2 and 5 million mesh elements were created in the ellipsoid. For the outer part of the domain, the minimum element size was set 0.001 and 0.05 for maximum and 1 million extra mesh elements were created. Mesh distribution is given in Fig. 1.

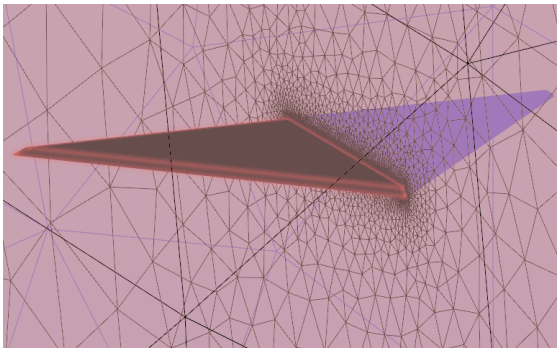

Figure 1. Delta wing for 6 million mesh.

RESULTS AND DISCUSSION

Simple delta wing with thickness 3 mm, chord length 101.6 mm, wingspan 254 mm, 30° beveled angle, and 40° sweep leading edge was numerically investigated by using SST $k-\omega$ turbulence model. The numerical calculation was performed with a server with 64 GB RAM and 32 processors. Fig.2 shows dye visualization experiment (Canpolat *et al*., 2009) the same configuration with the current study, which was conducted before at the angle of attack α=7°, 10°, 13°,17°. LEV and vortex breakdown are clearly visible at the angle of attack at 7°. When the angle of attack is increased to α = 10°, the location of the vortex breakdown moves upstream direction and reaches around x=0.5c. By the time α = 13°, the location of vortex breakdown moves toward the apex of the delta wing rapidly and flow shows significant fluctuations in the streamwise direction. At α = 17°, a large scale flow separation develops over the entire surface and flow passes to the stall stage completely (Canpolat *et al*., 2009).

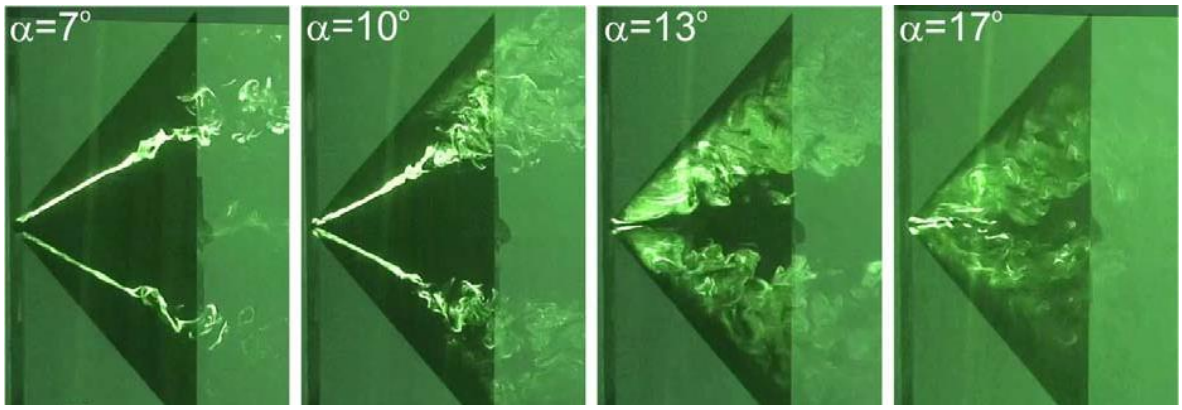

Figure 2. Dye visualization, development and formation of LEV, vortex breakdown (Canpolat *et al*., 2009)

.

Fig. 3 shows the streamline velocity field for the formation and development of LEV, the vortex breakdown, and the separated flow as a function of angle of attack angle from 5° to 17°. The LEV is clearly visible at the angle of 5° which is small in size and circulates along the downstream trajectory. When the angle of attack is increased to α = 7°, streamlines began to move away from each other and enlarge the rotating flow at the trailing edge side, indicating the onset of vortex breakdown. By the time α = 10° is reached (Fig. 3c), the flow continues to expand and rotate in the downstream trajectory and the location of the vortex breakdown moves to around x=0.5c. The dye visualization experiment in Fig.2 and Ref. (Yaniktepe and Rockwell, 2004) also confirm this numerical part (Fig. 3c) because, in the experiment, vortex breakdown starts at α=7° and moves to around at x=0.5c at the angle 10° and other numerical studies (Cummings *et a*l., 2008; Saha and Majumdar, 2012) confirm the streamline shape of the vortex breakdown. In the reported paper (Cummings *et al*., 2008) vortex breakdown happens likes streamlines are enlarging like a rotating cone. At α = 13°, the LEV system increases in size and strength with increased α and location of vortex breakdown moved to around apex, flow shows significant fluctuations in the streamwise direction, radius of rotation increased considerably but even if the flow structure is fluctuating, there is still continuing flow in the downstream and this implies that leading-edge vortex provides additional lift. The reported experiment in Fig. 3 (Canpolat *et al*., 2009 ; Yaniktepe and Rockwell, 2004) show that flow is not completely stalled at the angle of 13°and they correlate numerical results in Fig. 3(d). By the time the angle of attack reaches from α = 15° to 17°, downstream streamline structure deteriorates completely, location of vortex breakdown reaches to the apex and the flow passes to the stall phase as indicated in Fig. 2 (Canpolat *et al*., 2009).

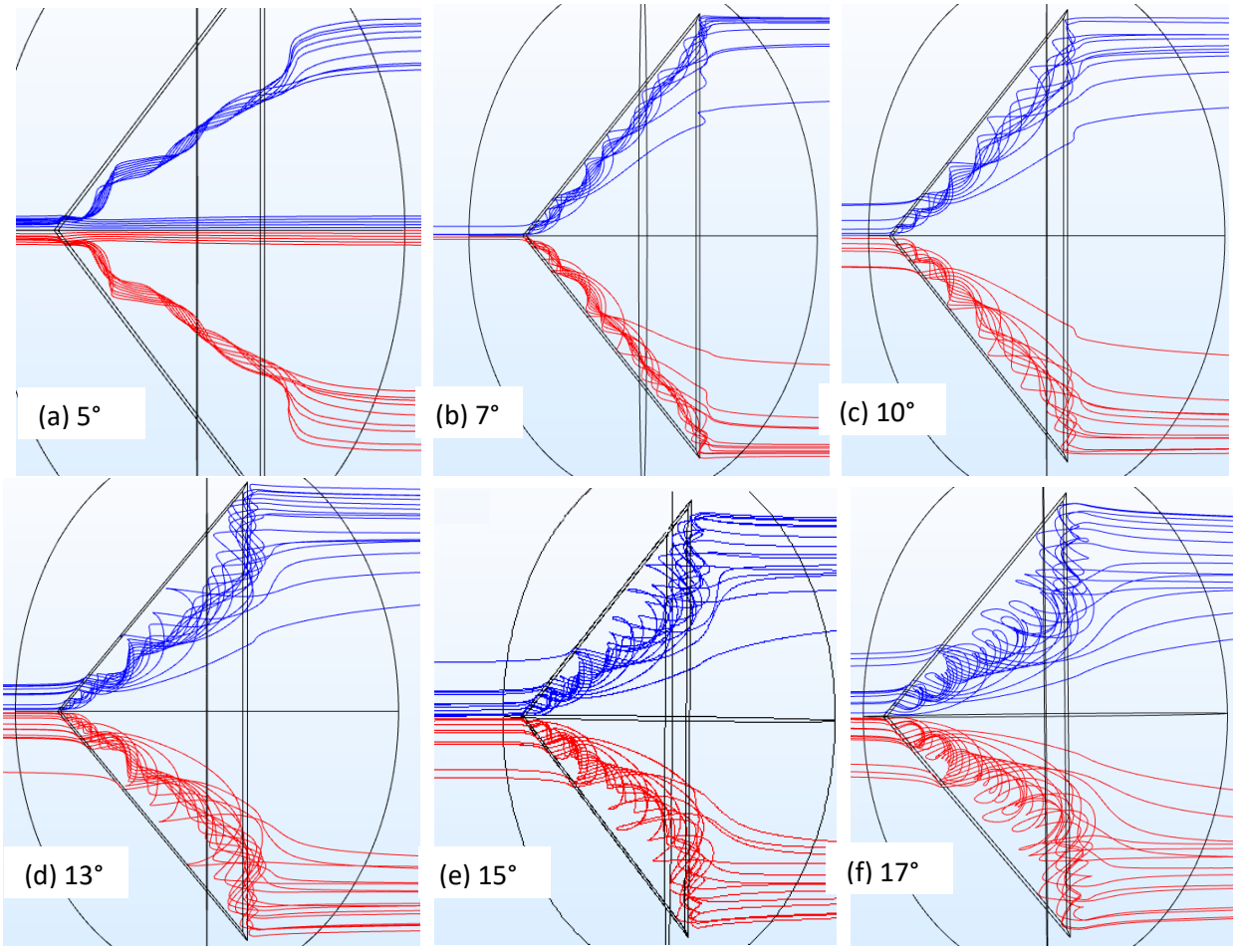

Figure 3.Lower surface plan view streamline velocity field (m/s)

.

Fig. 4 shows the vorticity magnitude contours of a delta wing at the angle of attack from 5° to 17°. Fig. 4a shows the development of small scale vorticity patterns. When the angle of attack is increased to 7°, there are three separate vorticity patterns as primary (PV), secondary (SV), and the third (VB). The primary rotating vortices occur in the inner side of the leading edge vortices which is close to the central axis of the delta wing and the secondary vortices develop between main vortex and side edges of the delta wing. It was reported in the previous experiment (Muir *et al*., 2017), if the secondary vortex is significantly weaker, which suggests breakdown. The development of a third stronger vortex indicates the onset of vortex breakdown (VB) at the middle backside of the wing. At α = 10°, the secondary vortex significantly disappears and the primary vortex increases in size and prolongs to the upstream direction. The area of vortex breakdown expands in all directions and flow shows significant fluctuations. At the angle of 13°, the vortex breakdown area increases and moves further upstream direction. Circulation of LEV is visible close to the apex but in other parts, the vortex breakdown prevails. By the time α = 15° is reached, the location of vortex breakdown moves further upstream but the flow hasn't completely stalled yet because there is circulation flow at the apex. Finally, by the time the angle of attack reaches α = 17°, the location of the vortex breakdown reaches the apex and the burst vortex slowly gives away to a largely stalled lower surface.

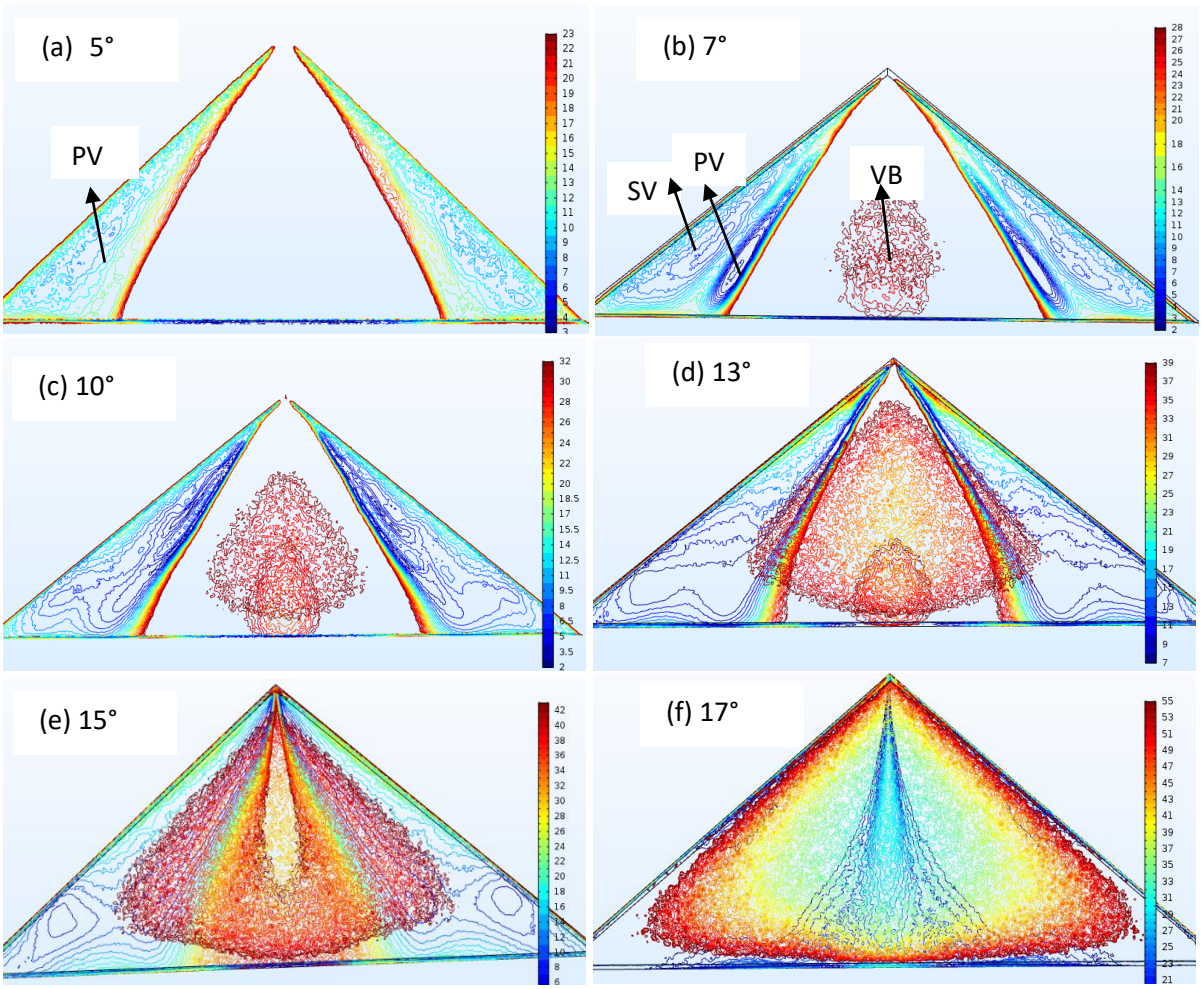

Figure 4. Plan view vorticity magnitude contour on the delta wing surface (1/s)

Fig. 5 shows PIV data (Yaniktepe and Rockwell, 2004) of the delta wing the same configuration with the current study. LEV starts to form very close to the lower surface by covering a larger area near the side edge at the angle of 7°. When the angle of attack increased to 13°, LEV becomes more pronounced, moves further down from the surface and approaches the centerline of the wing in the lateral direction. Finally, by the time angle of attack.

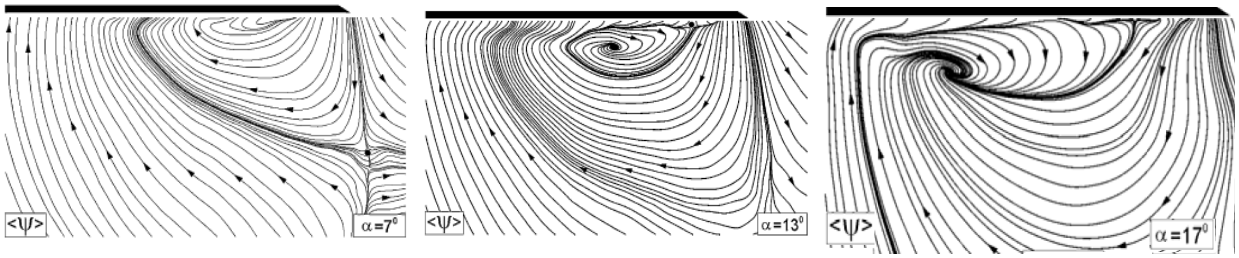

Figure 5. End view streamline velocity pattern (x/c=0.8) at the angle of attack at α=7°, 13°, 17° (Yaniktepe and Rockwell, 2004)

reaches α = 17°, LEV increases its intensity and continues its lateral and downward movement Fig. 6 shows the end view streamline topology at x=0.8C at the angle of attack from 5° to 17°. LEV formation starts very close to the lower surface at the angle of 5°. When the angle of attack increased, LEV becomes more pronounced, moves further down from the lower surface and also approaches the centerline of the wing in the lateral direction as indicated in the experiment (Fig. 5) (Yaniktepe and Rockwell, 2004). In contrast to the experimental measurements, the secondary vortex (SV) area was calculated. Secondary LEV is clearly visible at the angle of 7° and their size seems to become equal and tends to fade away at the angle of 10°. In line with the experiment (Muir *et al*., 2017) the secondary LEV shows the greatest reduction incoherence and this is an early indication of vortex breakdown. The presence of the secondary vortex was also confirmed for these two-angle cases (7° and 10°) in Fig. 4(b) and vortex core shifted down from the surface and also gets close to the centerline as the increasing angle of incidence.

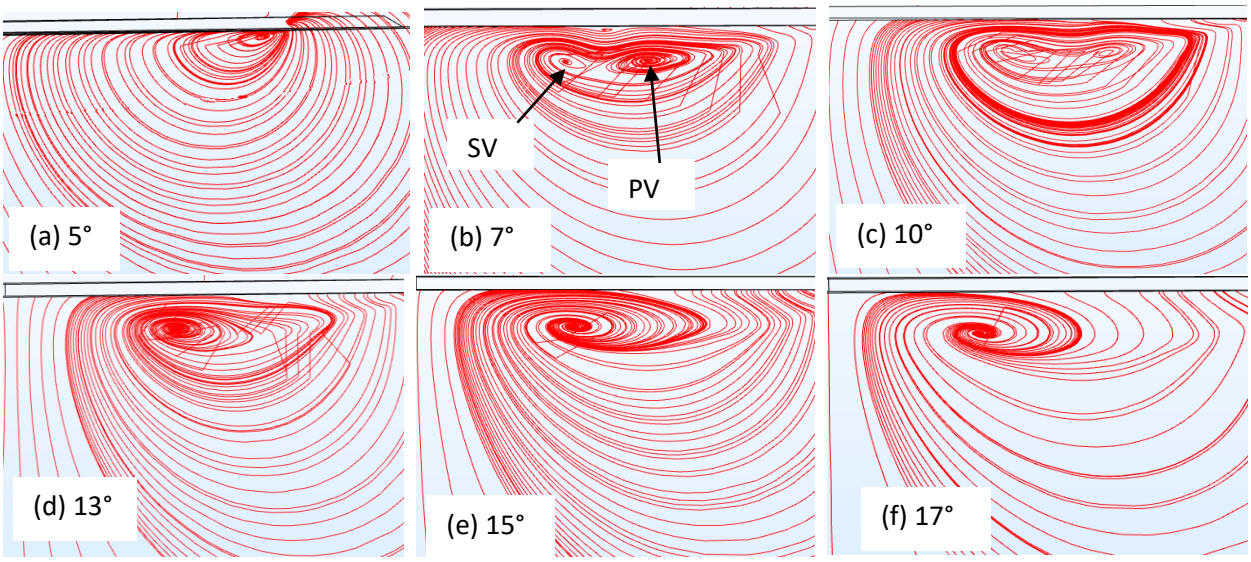

Figure 6. End view streamlines velocity field (m/s) at x/C= 0.8 when the angle of attack changes from 5° to 17°.

Fig.7 shows the end view velocity field magnitude with arrow and color range representation of the delta wing at the angle of attack from 5° to 17°. At the angle of 5°, a small size leading-edge vortex formation starts very close to the lower surface and lateral edge. As the increasing angle of attack, the size of LEV increases and moves close to the centerline. Secondary vortex is visible at the angle of 7° and 10°. By the time angle of attack reaches 13°, the severity of LEV increases and the core of cyclic vortex became more pronounced. When the angle of attack increased further up to 15°, vortex becomes more violent and vortices on both sides merged into a single vortex at the angle starting from 17°.

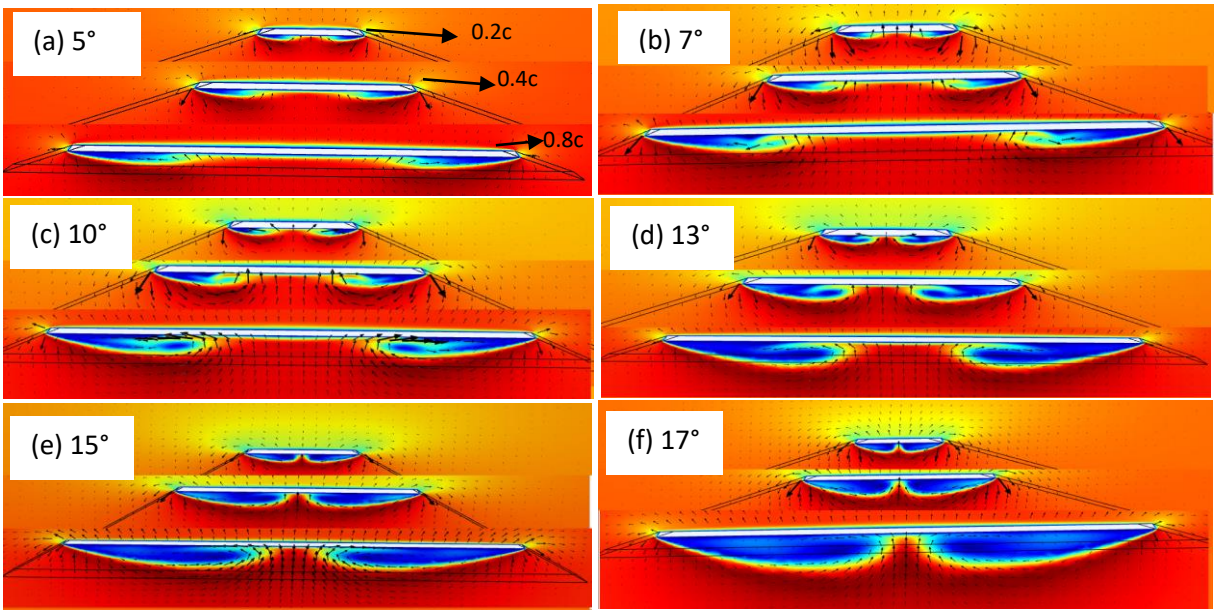

Figure 7. End view velocity field magnitude (m/s) with arrow and color representation; In the figure upper to lower x/C= 0.2, x/C= 0.4, x/C= 0.8, when the angle of attack changes from 5° to 17°.

Fig. 8 shows the end view vorticity contour magnitude at x/C= 0.8, where there are two vorticity patterns at α=5°. The smaller vortex is secondary LEV (SV) and it is very close to the bottom surface and the larger one is primary LEV (PV), located just below the small one, which spreads over the half surface of the wing. As the increasing angle of attack to 7° and 10°, secondary LEV lost its prominence and merged with the primary vortex and disappeared completely at 13°. Several small-scale vortex areas start to form within the primary vortex starting at the angle of 7° and numbers of them increase with the increasing angle.

This was also reported in a previous experimental study (Muir *et al*., 2017). An increasing number of small scale vorticity regions (SSVR) indicates the onset of vortex breakdown, because after breakdown numbers of small scale vorticity regions increases (Muir *et al*., 2017). Vortex breakdown location moves to upstream direction as the increasing angle of incidence and this increases turbulence at the backside of the wing. The numbers of small scale vortex regions increase up to the angle of 13° then start to decrease and finally they merge to become a single huge rotation core at α=17°.

CONCLUSION

This paper numerically investigates the effect of angle of attack on the aerodynamic performance of a simple delta wing by using CFD with the SST k-ω turbulence model and findings were compared with experimental observation to assess simulation accuracy of the Computational Fluid Dynamics (CFD) approach. Streamline velocity field and vorticity magnitude contour for plan and end view cases were investigated at the angle of attack from 5° to 17°, and the simulation results were compared with those obtained water channel experiment and comparison showed good agreement. First, the streamline velocity field was simulated for the plan view case. Leading-edge vortex developed at the angle of 5°, vortex breakdown started in the back lower side of the wing at α=7°. As the increasing angle of attack from 7° to 10°, the location of the vortex breakdown moved toward x=0.5c. The location of the vortex breakdown reached closed to the apex of the delta wing rapidly when the angle of attack increased to 13° and this was confirmed by reported experiment. There is no complete vortex breakdown at 13° because LEV is visible at very close to the apex but after 15°, the flow regime shows a complete deterioration and passed to the stall stage at the angle of 17°. Next, plan view vorticity magnitude contour on the delta wing was investigated and location and evolution of primary and secondary LEV and also vortex breakdown were analyzed for the angle of attack from 5° to 17° and compared with experimental observations. The secondary vortex system was identified at the angle of 7° and disappeared after 10°. Finally, end view streamlines velocity and vorticity field were investigated and discussed.

The application of CFD has accelerated the design process of the aerodynamic vehicle. Aerodynamicists could predict the flow properties of aircraft only by doing an experiment

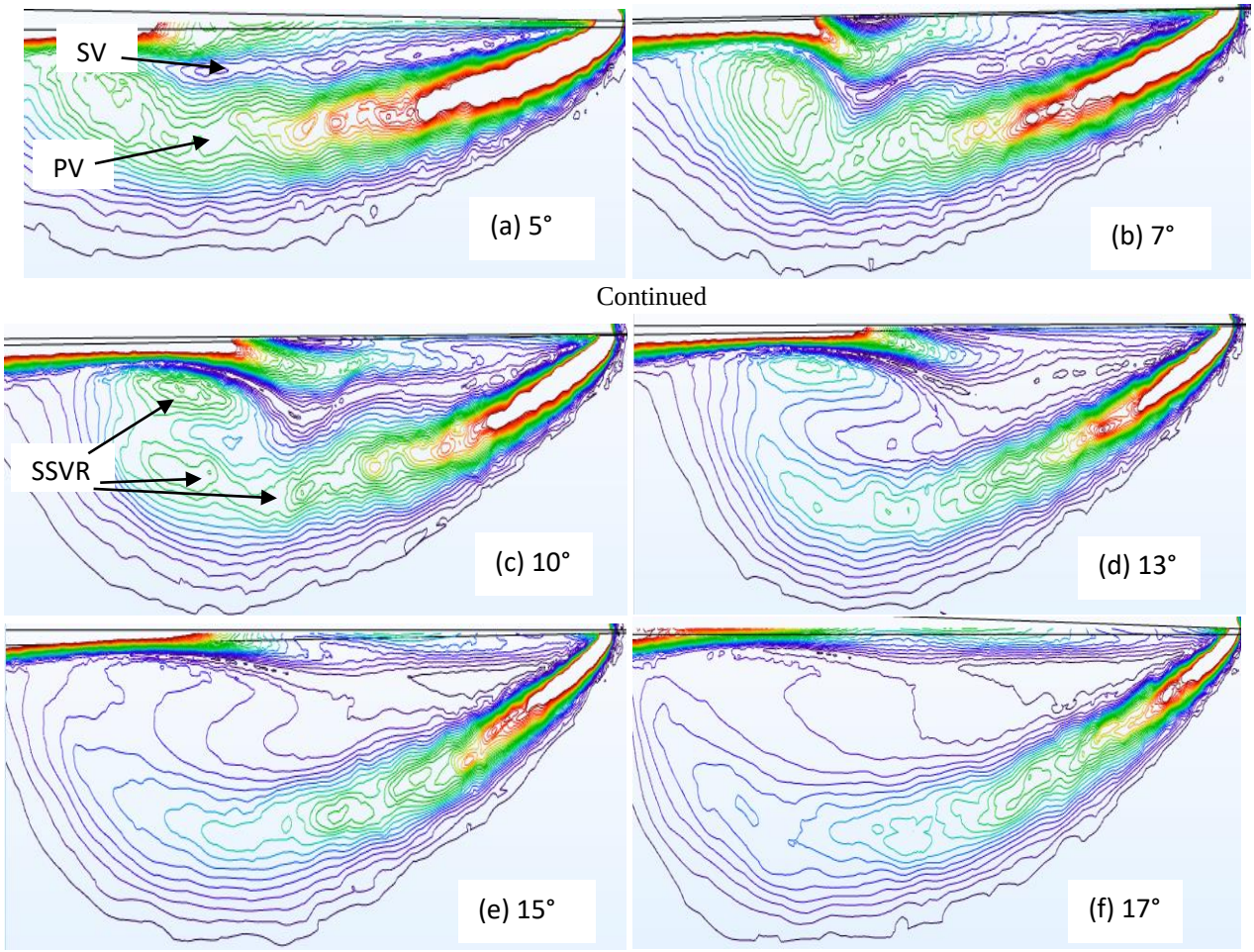

Figure 8. End view vorticity magnitude (1/s) contour lines at x/C= 0.8 when the angle of attack changes from 5° to 17°.

or by using an analytic method in a long time ego. However in the last 40 years, with the development of sophisticated computers, CFD has become a main supplementing tool to experiment. Because CFD is a cost-effective and critical tool to predict accurately and confirm flight characteristics of an object in any flow condition.

ACKNOWLEDGMENT

Many thanks to Middle East Technical University and Adiyaman University for technical support. This work was supported by Adiyaman University Scientific Research Project (Project no: TEBMYOMAP/2018-0001).

REFERENCES

Canpolat C., Yayla S., Sahin B., Akilli H., 2011, Observation of the vortical flow over a yawed delta wing, Journal of Aerospace Engineering, 25(4), 613-626.

Canpolat C., Yayla S., Sahin B., Akilli H., 2009, Dye visualization of the flow structure over a yawed nonslender delta wing. Journal of Aircraft, 46(5), 1818-1822.

Cummings R.M., Morton S.A., Siegel S.G., 2008, Numerical prediction and wind tunnel experiment for a pitching unmanned combat air vehicle, Aerospace Science and Technology 12(5), 355-364.

Cummings R.M., Schütte, A., 2013, Detached-Eddy Simulation of the vortical flow field about the VFE-2 delta wing, Aerospace Science and Technology, 24(1), 66-76.

Elkhoury M., Yavuz M.M., and Rockwell D., 2005, Near-surface topology of unmanned combat air vehicle planform: Reynolds number dependence, Journal of aircraft 42(5), 1318-1330.

Gordnier R.E., Visbal M.R., 2003, Higher-order compact difference scheme applied to the simulation of a low sweep delta wing flow, 41st AIAA Aerospace Sciences Meeting and Exhibit, 6–9 January, Reno, NV. AIAA 0620.

Gursul I., Gordnier R., Visbal M., 2005, Unsteady aerodynamics of nonslender delta wings, Progress in Aerospace Sciences, 41(7), 515-557.

Gülsaçan B., Şencan G., Yavuz, M.M., 2018, Effect of Thickness-to-Chord Ratio on Flow Structure of a Low Swept Delta Wing, AIAA Journal, 56(12), 4657-4668.

Johnson F. T., Tinoco E. N., Yu, N. J., 2005, Thirty years of development and application of CFD at Boeing Commercial Airplanes, Computers & Fluids, 34(10), 1115-1151.

Kyriakou M., Missirlis D., Yakinthos K., 2010, Numerical modeling of the vortex breakdown phenomenon on a delta wing with trailing-edge jet-flap, International Journal of Heat and Fluid Flow, 31(6), 1087-1095.

Mary I., 2003, Large eddy simulation of vortex breakdown behind a delta wing. International journal of heat and fluid flow, 24(4), 596-605.

Menter F.R., 1994, Two-Equation Eddy-Viscosity Turbulence Models for Engineering Applications, AIAA Journal, 32, 1598-1605.

Muir R. E., Arredondo-Galeana A., Viola I.M., 2017, The leading-edge vortex of swift wing-shaped delta wings, Royal Society open science, 4(8), 1-14.

OL M.V., Gharib M., 2003, Leading-edge vortex structure of nonslender delta wings at low Reynolds number, AIAA Journal, 41(1), 16–26.

Saha S., and Majumdar B., 2012, Flow visualization and CFD simulation on 65 delta wing at subsonic condition, Procedia engineering, 38, 3086-3096.

Sogukpinar H., 2019, Numerical Investigation of Influence of Diverse Winglet Configuration on Induced Drag, Iranian Journal of Science and Technology, Transactions of Mechanical Engineering, 44, 203-215.

Sogukpinar H., 2018, Low Speed Numerical Aerodynamic Analysis of New Designed 3D Transport Aircraft, International Journal of Engineering Technologies, 4(4), 153-160.

Taylor G.S., Schnorbus T., Gursul I., 2003, An investigation of vortex flows over low sweep delta wings, AIAA Fluid Dynamics Conference, 23–26 June, Orlando FL, AIAA 4021, 1-13

Wentz W.H., Kohlman D.L., 1971, Vortex breakdown on slender sharp-edged wings. Journal of Aircraft, 8(3), 156–61.

Yayla S., Canpolat C., Sahin B., Akilli H., 2010, Elmas Kanat Modelinde Oluşan Girdap Cokmesine Sapma Acisinin Etkisi, Isi Bilimi ve Teknigi Dergisi/Journal of Thermal Science & Technology, 30(1),79-89.

Yaniktepe B., and Rockwell D., 2004, Flow structure on a delta wing of low sweep angle, AIAA journal, 42(3), 513-523.

Yavuz M., Elkhoury M., and Rockwell D., 2004, Near-Surface Topology and Flow Structure on a Delta Wing, IAA Journal, 42(2), 332–340.

Internet, 2019, Pardiso Parallel Sparse Direct and Multi - Recursive Iterative Linear Solvers, User Guide Version 6.0, https://pardiso-project.org [accessed 20 February 2019].

Internet, 2019, COMSOL CFD module user guide http://www.comsol.com, [accessed 20 February 2019].

Haci SOGUKPINAR is an assistant professor at Adiyaman University, Department of Electric and Energy in Vocational School. He received his B.Sc. (2001) in Physics at Middle East Technical University, Ankara, Turkey, and his PhD (2013) in the Department of Physics at Eskisehir Osmangazi University. His research field is about computational fluid dynamics (CFD), heat transfer and also experiment related to fluid flow in the water channel. He has two books, one is related to the application of the COMSOL simulation technics and second book is related to industrial design with SOLIDWORKS and its applications and both books are available online sales.

SERKAN CAG is a teaching assistant at Adiyaman University, Department of Machinery and Metal Technology in Vocational School. He received his B.Sc. (2012) in Energy System Engineering and M.Sc. (2015) in Mechanical Engineering Department at Osmaniye Korkut Ata University, Osmaniye, Turkey. His research field: Flow Visualization and Control, Flow Topology, Flow Structure on Delta Wings, Vortex Breakdown.

BULENT YANIKTEPE is an associate professor in the Mechanical Engineering Department at Osmaniye Korkut Ata University. He received his B.Sc. (1998), M.Sc. (2000) and also his PhD (2006) in Department of Mechanical Engineering at Cukurova University Adana, Turkey. His research field: Flow Visualization and Control, Flow Topology, Flow Structure on Delta Wings, Vortex Breakdown**.**